Engineering Failure Analysis 17 (2010) 818–837

Contents lists available at ScienceDirect

Engineering Failure Analysis

journal homepage: www.elsevier.com/locate/engfailanal

Failure analysis of natural gas pipes

Z.A. Majid [a,*], R. Mohsin [a], Z. Yaacob [a], Z. Hassan [b]

[a] Gas Technology Centre, Universiti Teknologi Malaysia, 81310 Johor, Malaysia
[b] Faculty of Chemical & Natural Resources Engineering, Universiti Malaysia Pahang, 26300 Pahang, Malaysia

ARTICLE INFO

Article history:
Received 15 July 2009
Accepted 9 October 2009
Available online 15 October 2009

Keywords:
Pipeline
Slurry erosion
Erosion–corrosion
Natural gas pipe
Failure analysis

ABSTRACT

Incident involving failures of 6 months old API 5L X42 (NPS8) and SDR 17, 125 mm medium density polyethylene pipe (MDPE) supplying natural gas to an industrial customer has caused serious 7 h supply disruption. Study was performed to identify the most probable cause of the pipes failures. The study conducted by reviewing the existing design and construction data, visual physical inspection, pipe material analysis, structural analysis using NASTRAN and Computational Fluid Dynamics analysis (CFD) using FLUENT. Investigations revealed that high pressure water jet from leaked water pipe had completely mixed with surrounding soil forming water soil slurry (high erosive properties) formed at a close vicinity of these pipes. Continuous impaction of this slurry upon the API 5L X42 pipe surface had caused losses of the pipe coating materials. Corrosion quickly ensued and material loss was rapid because of the continuous erosion of oxidised material that occurred simultaneously. This phenomenon explains the rapid thinning of the steel pipe body which later led to its failure. Metallurgical study using photomicrograph shows that the morphology of the steel material was consistent and did not show any evidence of internal corrosion or micro fractures. The structural and CFD simulation results proved that the location, rate and the extent of erosion failures on the pipe surfaces can be well predicted, as compared with actual instances.

1. Introduction

Cases involving failure of pipes carrying highly combustible fuel such as natural gas are rarely reported. High pressure natural gas transmission pipeline (API 5L X60) in northern part Pakistan [1] and a T-shape natural gas pipeline network (API 5L X52) near gas extraction plant in northern Mexico [2] are two examples of such cases. In both cases the material degradation causes by corrosion is the main factor that contribute to the failure of the pipes. Another example of a similar pipes but carrying liquid fuel that has failed are the 52 km 16″ (406.4 mm) pipe (API 5L X52) in Kuwait [3] and the API 5L X46 pipe in Brazil [4]. Delayed cracking and transverse cracking has been identified as a reason for the pipes to fail.

A case involving the failure of natural gas pipes adjacent to water is yet to be reported. A leak of high pressure water pipe in a mixture of soil and sand can create an erosive slurry impact on nearby pipes. Slurry erosion will form by the interaction of solid particles suspended in liquid and a surface which experience losses of mass by repeated impacts of particles [5]. This type of erosion has been reported as the major source of failure of many engineering equipment such as slurry equipment and hydraulic components [6–8].

This erosive slurry impact will cause metal loss or metal thinning and eventually lead to the pipe failure [5]. This event could trigger much disastrous incident involving fire and explosion which could cause loses in term of life and economics [9,10].

* Corresponding author. Tel.: +60 7 5535574; fax: +60 7 5545667.
E-mail address: zulmajid@fkkksa.utm.my (Z.A. Majid).

1350-6307/$ - see front matter © 2009 Elsevier Ltd. All rights reserved.
doi:10.1016/j.engfailanal.2009.10.016

2. Background of the incident

The location of the gas pipe leak was evident after the personnel from a gas utility company in northern part of Malaysia observed the bubbling of the gas through the watery soil (Fig. 1). Prompt action was taken where the leakages were immediately isolated through valves. A team was later sent to excavate the site at the incident area. This was carried out in order to locate the exact source of the leakage, to rectify and repair the damaged pipes and to make a proper record of the failure or damage for further investigation. Presented in this paper are findings, probable cause of failure and conclusions concerning the failure of the pipes.

3. Methodology

Studies conducted were comprised of four fundamental aspects. First, the background information which caters in the form of design and construction data that provide basic formation for understanding the sequence of events and operational conditions that might have led to the failures of the pipes. This studied was later followed by physical inspection of specimen, recorded photos and subsequent observation of the actual failed pipes sections. This has been conducted in order to locate the actual position and orientation of pipes and to reconstruct the event that lead to the failure. Next, the metallurgical analysis of pipes was performed on the pipe section and its surrounding failure area, followed by final study on the structural and flow propagation. The structural analysis will provide insight of the stress distribution in the vicinity of the failed pipe section as thinning occurs. Therefore, the location and weakness area can be well predicted. The CFD analysis conducted could provide simulation of graphical velocity and pressure profile of the leakage and bursting analogy. It could also indicate how it might have affected or lead towards the failure of the adjacent pipe/s.

4. Findings and discussion

4.1. Review of background information

Upon the discovery of the incident location area, it was evident that three pipes adjacent to each other; a 8″ (203.2 mm) steel NPS8 and a 125 mm MDPE natural gas pipes, and a 6″ (152.4 mm) asbestos water pipe lying parallel to each other, with all three indicating signs of damage or leak. An electrical cable lying parallel to the pipes with no apparent sign of damage also presence in a close vicinity. The NPS8 and MDPE pipe was carrying natural gas at about 1800 kPa and 345 kPa pressure, respectively, prior to shut down. The asbestos pipe was transporting water with an estimated flowing pressure of 1000 kPa (10 bar).

The failed NPS8 gas pipe was made of carbon steel manufactured with specification of API 5L X42. It was buried 1.3 m below the ground about 195 mm laterally from the underground water pipe. The water pipe was buried at a similar depth. Slightly above it, at 1.2 m below the surface and at roughly the same distance between the steel pipe and the water pipe, is the MDPE gas pipe (Fig. 2). The thickness of the NPS8, MDPE and asbestos pipe were 5.6 mm, 11.4 mm and 10 mm respectively (see details in Table 1).

There were four possible reasons initially given as the possible root cause of the failures, which are:

i. Construction defect.
ii. Third party damage.

Fig. 1. Surface water splashing due to gas pipe leakages.

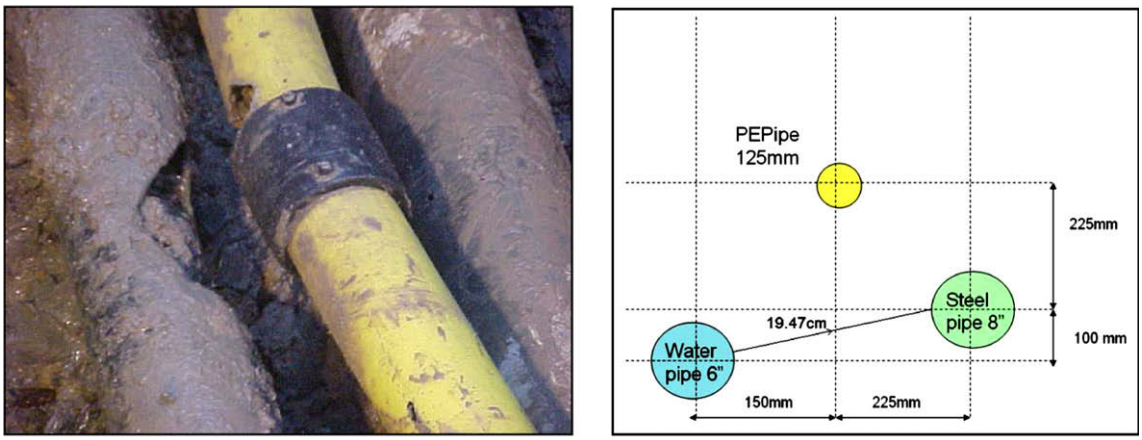

Fig. 2. Relative positions of API 5L X42, 6 in. asbestos and PE pipes.

Table 1
Physical parameters of pipes.

Parameters	NPS8 gas pipe	PE gas pipe	Water pipe
Depth cover (m)	1.3	1.2	1.3
Material	Carbon steel	Polyethylene	Asbestos
Internal diameter (mm)	203.2	102.2	152.4
External diameter (mm)	214.4	125.0	172.4
Thickness (mm)	5.6	11.4	10.0
Fluid pressure (KPa)	1800	345	1000

iii. Pipeline material defect.
iv. Leaking water pipe impact.

It is made to understand that the pipeline was laid about six months prior to the incident. Standard construction procedures that require proper coating, sound cathodic protection system and other pipeline integrity measures has been appropriately complied during construction and pipe laying process. This diminished the possibility of the construction defects.

On the possibility of third party works or acts, initial discussion with the gas utility company personnel and available operational records dismissed that this had taken place. Furthermore, visual inspection did not find any indication or evidence to support this fact. To answer the third possibility, the metallurgical analysis was subsequently performed and will be discussed details in the following section.

Visual inspections were carried out on both the photos and on the two physical pipe specimens provided (Fig. 3). When received, the exposed part of the steel pipe (with the coatings eroded) is already heavily oxidized (Figs. 3a and 4a). Only when the photo records were received, was the original condition of the exposed part, immediately after the incident, became evident. It was found that the coating materials has been completely stripped was in fact clean, smooth and shiny (Fig. 4b).

The pipes were later rearranged in the lab to reconstruct the positioning of each pipe relative to each other prior to the failures. This was conducted based on the original information supplied. The repositioning of the pipes was important to help us to build a better understanding on the direction of the leaks and how it might have impacted upon the adjacent pipes (Fig. 5).

On the NPS8 carbon steel pipe section, a hole with an average diameter of 10 mm was discovered in the middle of the eroded part of the pipe (Fig. 6). The eroded part was found to be smooth and free from the rust. The size of the eroded section was around 50 cm by 30 cm (Fig. 4b). The absence of scratch marks or dents in the vicinity of the eroded part seem to support the statements of site engineers that no third party work was being observed at the location of incident.

Our initial assessment suggests that the asbestos water pipe with 10 mm wall thickness was the first to fail. The flowing water pressure in the pipe was reported to be around 1000 kPa (10 bar). The leak could have caused a high pressure water jet which, with the presence of the surrounding soil and sand materials, could have produced highly abrasive slurry. This slurry could have initially impacted upon the NPS8 causing the erosion of the coating materials followed by thinning of the steel pipe body. After sufficient pipe material was removed, the remaining pipe strength will no longer be able to withstand the high internal pipe pressure. This eventually led to the steel pipe rupture and enlargement of leak section.

a. API 5L X42 pipe b. SDR 17 PE 125 mm pipe

Fig. 3. Photos of two failed specimen.

a . API 5L X42 is heavily oxidized b. API 5L X42 pipe after the incident

Fig. 4. Surface condition of failed steel pipe.

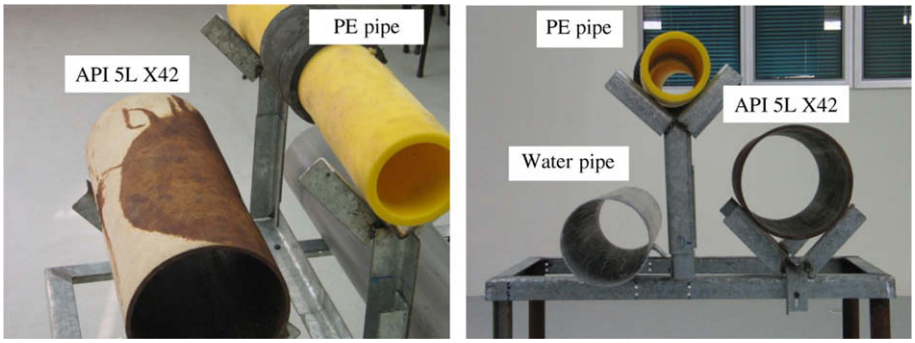

Fig. 5. Reconstruction of relative original pipe positions.

The high pressure jet of leaked water from the water pipe had earlier caused the displacement of the supporting soil materials underneath the MDPE pipe causing it to move downwards. When the steel gas pipe leaked, more materials were

a. Overall view of a hole b. Closed up view

Fig. 6. 10 mm diameter of hole on API 5L X42 pipe.

displaced causing the MDPE pipe to drop even further until it was low enough to be '*in the line of fire*' from the high pressure gas jet (Fig. 7).

The visual inspection of the photos of the incident and on the damaged pipe sections led to early conclusion that the source of damage to polyethylene pipe (MDPE) is due to the high pressure impact of the gas jet which originates from the carbon steel pipe (NPS8) leak. This is most evident from the final location of the MDPE pipe relative to the NPS8 pipe leak and the erosion pattern found on the MDPE pipe damaged area (Figs. 7 and 8). Thus the metallurgical and structural analysis is only required for the NPS8 carbon steel pipe.

4.2. Analysis on pipe's failed section

Visual assessment of the position of the damaged part of PE pipe relative to the steel pipe leakage led us to conclude that the PE pipe damage was directly caused by the impact of the high pressure (1800 kPa/18 bar) gas jet that gushed through. Therefore, the metallurgical/physical analysis of the pipe failure was only conducted for the NPS8 pipe. Analyses of the steel pipe failure include the following tasks:

i. Visual examination of steel gas pipe and photography.
ii. Dimensional mapping of the failed gas pipe.
iii. Metallographic analysis on the failed steel pipe using optical microscopy.

4.2.1. Visual examinations

The carbon steel gas pipe was inspected externally and internally and photo-documented. The examination of the gas pipe revealed the following facts:

Fig. 7. In-situ PE pipe directly 'in the line of fire' of the API 5L X42 gas jet.

Fig. 8. Repositioned of API 5L X42 and PE pipe in lab (after excavation) truly match with Fig. 7.

i. The NPS8 gas pipe has a hole on the surface facing the water pipe measuring 11 mm × 9 mm shown in Fig. 6b.
ii. The side of gas pipe facing the water pipe and where the hole is located has lost its coating completely and exhibited a clean and shiny surface as shown in Fig. 4b and Fig. 6a.
iii. No significant scale or deposit was noted on the inside surface of the pipe indicating no internal corrosion.

4.2.2. Dimensional mapping

Dimensional mapping was conducted on the two half circles, where the hole is located, about 50 mm apart as shown in schematic diagram in Fig. 9. Results are illustrated in Fig. 10a–c for specimen A and specimen B, respectively. Results obtained clearly showed that the thickness of the metal decreased substantially closer against the jetting orifice position. In other words, metal loss has occurred on the area facing directly to the water pipe orifice jet resulting in a hole which increased in its dimensional size with severed metal losses. This indicates that the hole was caused by drastic erosion probably from the failed water pipe buried in the vicinity of the gas pipe.

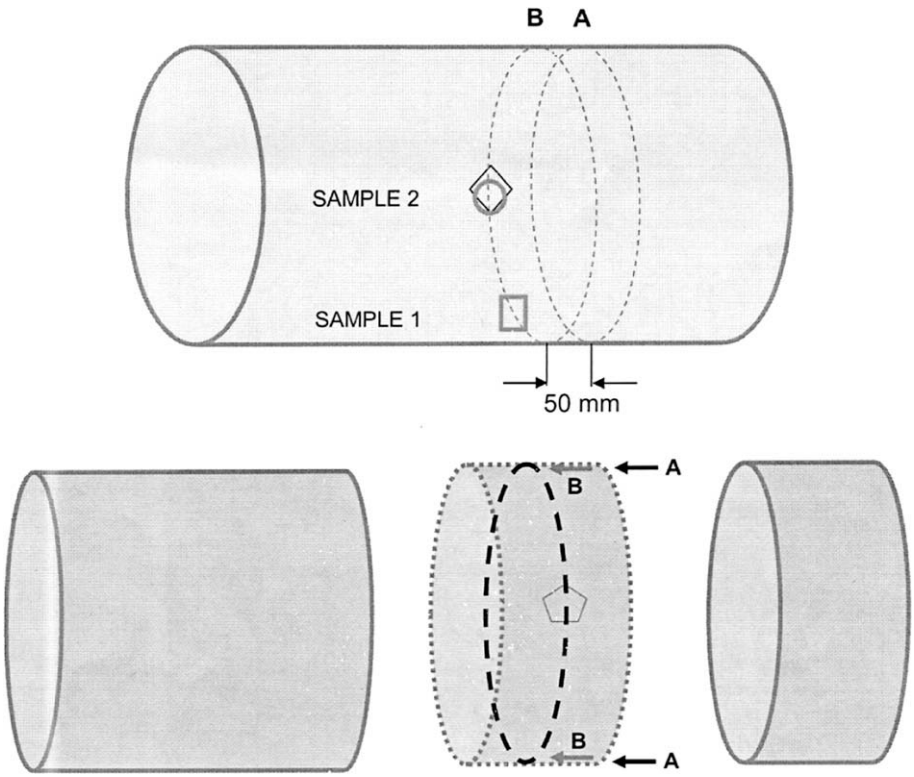

Fig. 9. Schematic of steel gas pipe showing procedures of dimensional mapping and specimen preparation.

4.2.3. Microstructural analysis

Mechanical and operating data of the pipeline are summarized in Table 2. The pipe had been strictly manufactured to follow API 5L X42 requirement. The pipeline has been tested hydrostatically at the mill for 15100 kPa (151 bar) on August 3rd 2003. Table 3 shows the chemical composition of the pipe.

Microstructural examination of the gas pipe was undertaken to determine possibility of microstructural deficiencies of the pipe at the failure region. If the results reveal consistency of microstructural arrangement at the failure region compared with another section away from the failure (considered as the base metal), then it can be concluded that erosion is the main cause of the pipe failure.

This task was carried out by microstructure examination of two specimens at location away from the leak hole (specimen 1) whilst another specimen was taken at the failure area (specimen 2) in the same plane shown in Fig. 10a and b. Prepared specimens were then examined with 200X magnification using Nikon optical metallographic microscope.

Examination of the microstructure at the failure region and base metal location clearly indicate close similarity between specimen 1 and specimen 2 that consists of the typical ferrite and pearlite structure observed in carbon steels. There is also no evidence of any micro fractures. The microstructures are shown in Fig. 11a–d for respective specimen 1 and specimen 2. These findings fully support earlier hypotheses that the pipe was failed due to the erosion of pipe surface instead of corrosion.

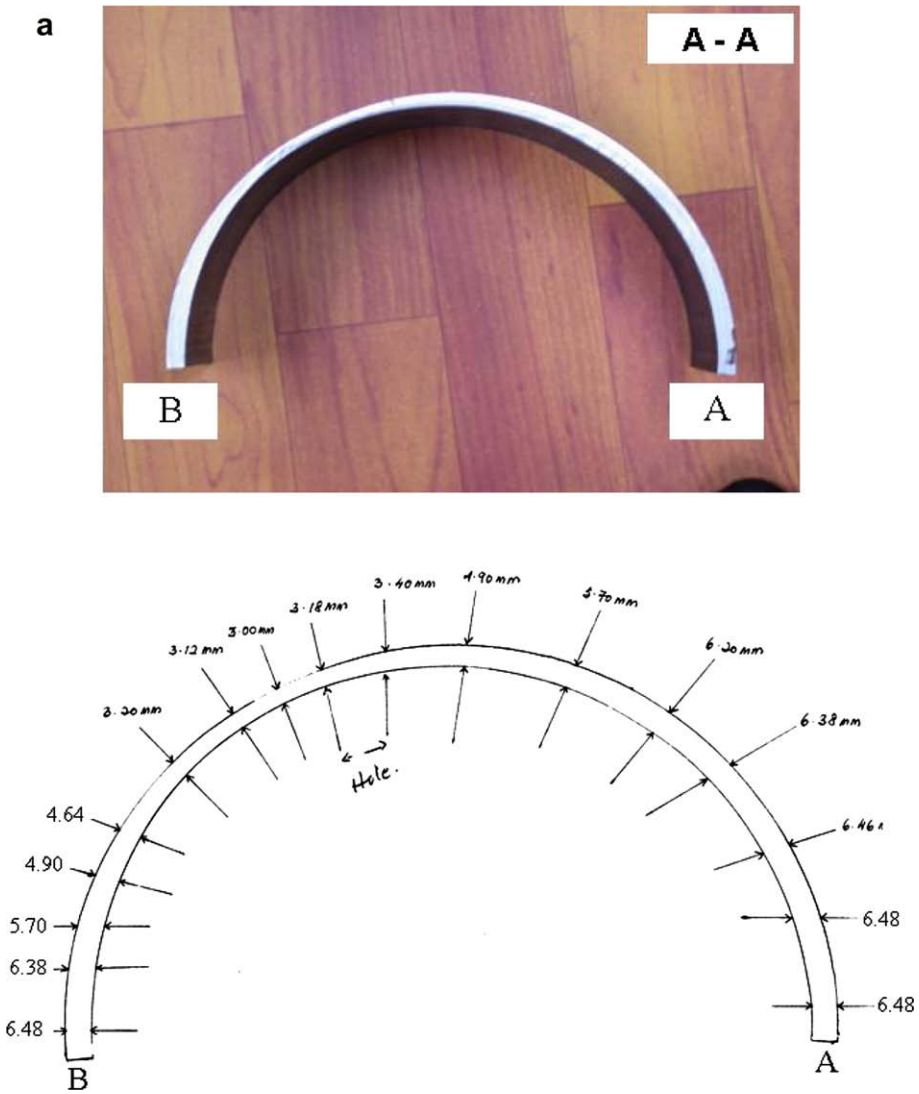

Fig. 10. Dimensional mapping of API 5L X42 gas pipe. (a) Results of dimensional mapping for section A – A (50 mm away from hole). (b) Results of dimensional mapping for section B – B (half way through the hole). (c) Physical mapping at failure section B – B.

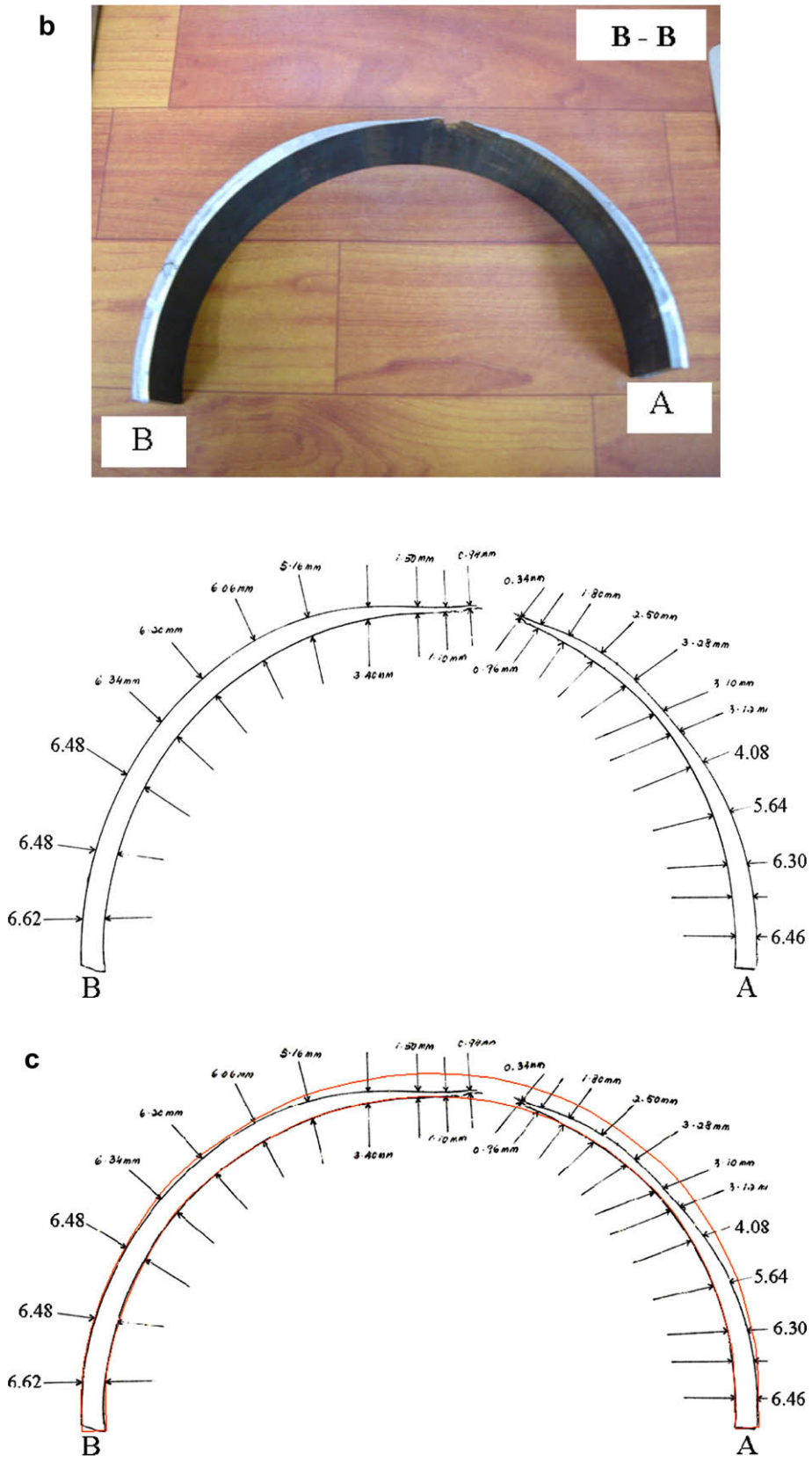

Fig. 10 (*continued*)

Table 2
Mechanical and operating data of pipeline.

Grade of steel	API 5L X42 42,000 psi min, yield
Type of pipe	Seamless
Material	Black carbon
Diameter	219.10 mm
Wall thickness	5.6 mm
Hydraulic pressure (factory tested)	15100 kPa

Table 3
Chemical composition (wt.%) of gas pipeline.

Sample													
C	Si	Mn	P	S	Cu	Cr	Ni	Mo	Ti	Co	B	Ca	Al
0.18	0.22	0.84	0.013	0.004	0.03	0.07	0.02	0.01	0.001	0.06	0.0001	0.00023	0.03

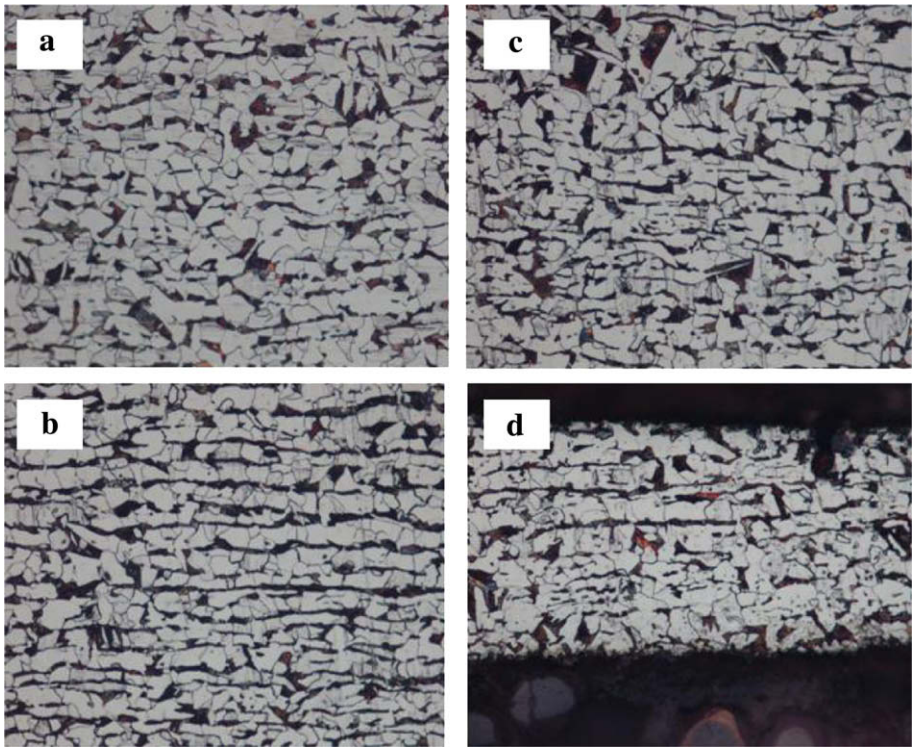

Fig. 11. Microstructures of the pipe taken from sample 1 (microstructure a) and sample 2 (microstructures b, c and d). There is no evidence of microstructure changes.

5. Probable cause of steel pipe leak

There are two possible scenarios that might take place, first, the NPS8 first to fail and cause the PE and water pipe to leak. This possibility could occur if contributed by the third party damage, construction faulty or due to material defects but it does not correlate with coating and material loss pattern.

Second scenario would be the water pipe first to fail. Small crack could have allowed strong jetting effect. This heavy jetting will mixed thoroughly with surrounding soil to produce corrosive slurry. This corrosive slurry erodes the coated pipe causing the coating losses that probably lead to surface oxidation/corrosion. With continuous direct water/slurry jet impact to the pipe could led to rapid pipe thinning, and finally pipe rupture. High pressure jetting from leaked water from the water pipe had earlier caused significant displacement of the supporting soil materials underneath the MDPE causing it to move downwards to a maximum displacement of around 200 mm, where it was impacted by the high velocity/pressure gas jet from NPS8 pipe.

6. Simulation study

6.1. CFD simulation

In this particular study, the FLUENT software was used to simulate the sequence of processes that might have taken place which led to the failure of the gas pipes. Results obtained from simulations reinforce the hypothesis made earlier, that the steel pipe leak was caused by the impaction of erosive soil water slurry from water pipe. As for the MDPE pipe, damages was then caused by the high pressure gas jet from the leak of the 1800 kPa (18 bar) NPS8steel pipe. Simulation conducted had ability to obtain pressure and velocity profiles surrounding impinged MDPE pipe. The information on how the gas jet flows from steel pipe behaved within the region is essential to strengthen the determination of the whole case study. Values obtained would assist structural simulation to model relevant boundary condition. In this particular study, two dimensional CFD analyses had been conducted.

The outlet is assumed to be exactly tangent to the steel pipe. Due to high velocity gas jetting with homogeneous resistance domain, jetting direction is expected to be in similar planner, thus two dimensional (2D) analyses is considered sufficient.

The pre-processing included physical modeling, setting-up appropriate boundary condition and construction of the computational mesh. Around 50,000 computational nodes (Fig. 12) were built and found to be sufficient in resolving computational domains. Boundary conditions that relate to geometric entities set up for this particular work are shown in Table 4.

In the water jet simulation, the operating pressure was set consistently 10 bars (1000 kPa). Gas jet flow is strictly restrained, since the primary intention of this part of the simulation is to obtain the flow behavior and its relevant flow profile effects to the steel pipe structure.

In simulating natural gas jetting, the system operation has been classified as compressible flow type. Hence, heat energy coupled with flow energy model was used. In order to simplify the modeling process, only steady condition was applied. Under the steady condition, it was assumed that computational domain is fully immersed in homogeneous water distribution. Slurry effect (water + soil) was not modeled due to lack of information on the soil physical characteristics.

The properties of water and methane were incorporated in the modeling. Methane which makes up more than 90% of the natural gas composition is assumed to be representative of the natural gas properties. Gravitational effect must be included since the movements of water within the region are highly dependent to its body relative force. Water flow was not being considered at this particular stage. This is due to nearly equilibrium region (nearly saturated) was reached between the domain which is flooded with water.

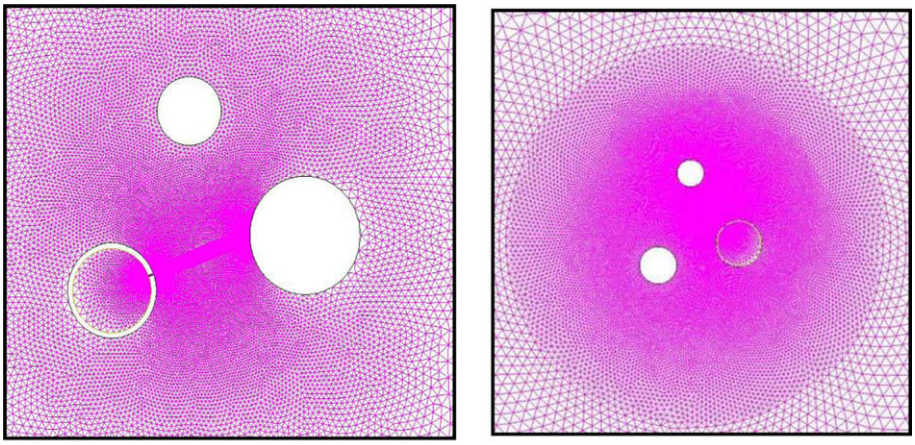

Fig. 12. Computational mesh for water jet and natural gas jet.

Table 4
List of boundary conditions.

Boundary type	Boundary conditions	
	Steel pipe jet	Asbestos pipe jet
Pressure inlet	Gas inlet (18 bar)	Water inlet (10 bar)
Pressure outlet	Ambient (0 bar)	Ambient (0 bar)
Wall	Pipe wall (adiabatic)	Pipe wall (adiabatic)
Symmetry	Left, right, bottom bound	Left, right, bottom bound

Gas flow leak from MDPE pipe has not been considered. Eventually it was earlier concluded that the MDPE pipe failed due to high gas jet impingement from the steel pipe rupture. Due to the high gas jet pressure of NPS8 pipe, the MDPE was expected to experience immediate failure. The failure of the MDPE pipe should not affect other pipes. Jet flow produced by the MDPE pipe section is considered weak due to its large failure outlet (Figs. 3b and 8).

6.1.1. Simulation hypotheses and assumptions

Through analysis of the case has enabled us to produce several hypotheses, prior to execute the flow simulation:

i. As the water pipe made of asbestos material, its brittle characteristic would cause the pipe to fail instantly. There will be no significant physical outlook left on the failed edge region. However, it was noticed from the photo taken from the site showing the upper part of the asbestos pipe seems experienced more failure than the lower part.
ii. The photo in Figs. 2, 5, 13 and 14 seemed to support the hypothesis that the water jet direction was around 20° from the horizontal axis. The 20° of jet flow direction was determined through ideal geometrical approached by assuming the jet flow direction was normal to the surface of the outlet (normal impaction). Exact initialization and condition of the asbestos pipe failure cannot be determined due to unavailability of asbestos water pipe specimen.
iii. MDPE pipe vertical position tends to be lowered (moving downward) due to lack of tangential support.
iv. As the medium was moving due to the jet flow from water pipe and steel pipe, MDPE pipe began to drop due the gravitational force and subsequent soil weight that vertically act on the MDPE pipe section (Fig. 15).
v. Asbestos water pipe and natural gas steel pipe were assumed not being displaced due to their physical stiffness.
vi. Once the MDPE pipe began to displace, in-equilibrium force acting on the PE pipe will occur.
vii. Expected operating strength of the MDPE pipe will reduce.
viii. From the existing design specification and sample of MDPE pipe, it was expected that the MDPE pipe would displace vertically around 225 mm away from its original position.

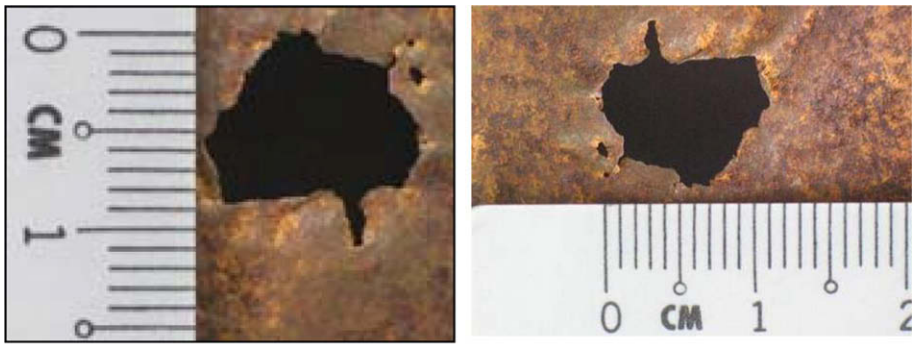

Vertical Hole Size Horizontal Hole Size

Fig. 13. Leak size on the NPS 8.

Fig. 14. Damaged asbestos pipe (water pipe).

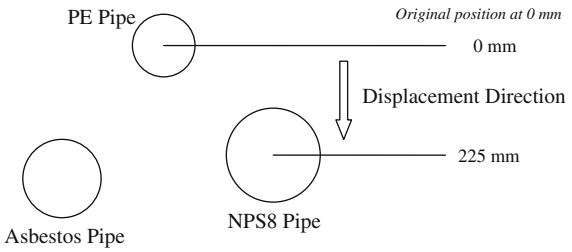

Fig. 15. Schematic of PE pipeline displacement.

6.1.2. Simulation results on water pipe leakage

The results for the simulation of water pipe leak are given in the picture sequence shown in Figs. 16 and 17. The possible sequence of events is as follow:

i. Failure started as a small crack, possibly longitudinal in direction. The simulation was initiated when the crack size has an effective diameter of 1.5 mm. The flow trajectories of the jet are shown in Figs. 16a and 17a.
ii. As the effective diameter increased to 3.0 mm, it was shown that the force of the jet impacting on the steel pipe surface was getting much more significant (Figs. 16b and 17b). It was strongly believed that the water/slurry were strong enough to cause coating losses on the steel pipe surface.
iii. The flow trajectory was also shown to move along the upper surface of the steel pipe. This fact supports the finding of the metallurgical study which shows a faster thinning process took place on the upper part of the pipe (Fig. 10c). This phenomenon totally agreed with the study conducted on cylindrical specimen using slurry pot erosion tester as shown in Fig. 18 [11].
iv. The simulation results seem to agree with the observed conditions of the pipe surface conditions as shown in Figs. 4b and 6a.

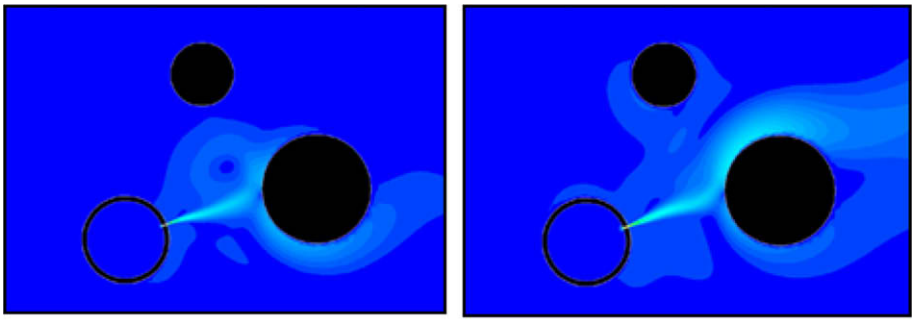

a. Hole size ≈ 1.5 mm b. Hole size ≈ 3.0 mm

Fig. 16. Result of water jet simulation (2D velocity profile).

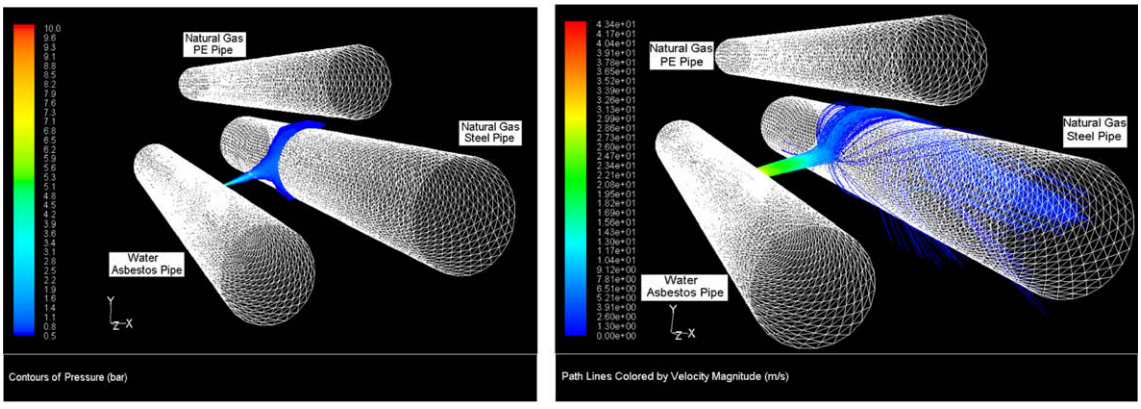

a. Hole size ≈ 1.5 mm b. Hole size ≈ 3.0 mm

Fig. 17. Result of water jet simulation (3D velocity profile).

6.1.3. Simulation results on NPS8 pipe leakage

The results for the simulation of the NPS8 pipe leak in term of pressure and velocity contour are given in the picture sequence as in Fig. 19a and b, respectively.

The following are the discussion of the probable cause and events that may had occurred as the MDPE pipe moves downwards (Fig. 15) due to the displacement and loss of supporting underneath materials, brought about by the continuous water and natural gas jetting streams.

Locating around 0 mm, 25 mm, 50 mm, 75 mm and 100 mm of subsequent vertical displacement, pressure contours showed that the pressure behaviour was not affected by the downward movement of the MDPE pipe, while the velocity contours show no significant differences. Jet flow from the leaked steel pipe tends to flow and diffuse as expected.

As the MDPE pipe further displaced to around 125 mm, it was clearly noticed that the pressure flow tends to change its direction. This was due to the direct perturbation of existing MDPE pipe close to regimes causing external aerodynamic obstruction. The upper side of the jet flow tends to move slower relative to the bottom side. Vorticity flow will further develop due to the differences of velocity difference between this opposite sides (Fig. 20).

This may have resulted due to different media contact phenomenon that contribute to external shear force created at the upper side of the jetting regions and gravitational forces that may also appears to this regime. After certain distance, it was noticeable that the flow directions diverge upward due to apparent physical obstruction by MDPE pipe and natural gas lower specific gravity.

As the MDPE pipe dropped vertically around 150 mm, the gas jetting direction directly hit the MDPE pipe, thus start to shear by the high impact high pressure gas jet flow. The pressure at this stage was around 1.7 bars with its flow velocity around 400 m s^{-1}. Fig. 17 indicated that the MDPE pipe may had experienced rapid failures.

6.1.4. Summary of CFD study

The MDPE pipe failed mainly because of its severe physical surrounding conditions. Based on thorough technical specification evaluation, physical observations made during the study period and direct computational simulation results it can be summarised that:

i. Water pipe leakages tends to flow continuously towards the steel pipe and causing shearing phenomenon to the steel pipe surface which directly contributed to the steel pipe failure.
ii. Results obtained indicate that, as the MDPE pipe vertical displacement does not exceed 100 mm, no significant effect to flow condition towards MDPE pipe surface due to water high speed flow.
iii. As the MDPE pipe lowered to 150 mm, significant contact between gas jet and the MDPE pipe external surface occurred and hence its surface would be directly subjected to shearing action of impacting flow.

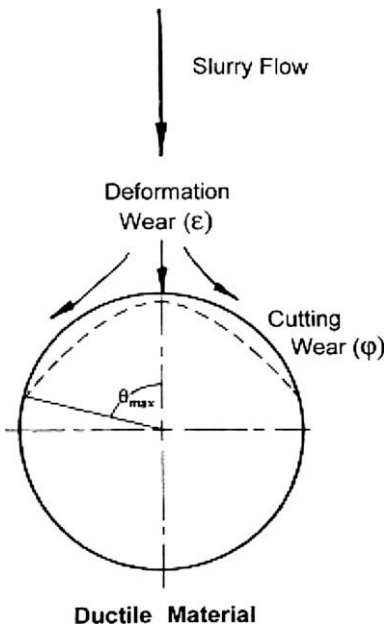

Fig. 18. Schematic diagram of slurry flow and distribution of deformation wear and cutting wear on a ductile material.

6.2. Structural simulation study via finite element analysis (FEA)

In this particular part of study, the NASTRAN software had been used to simulate and evaluate stresses around the steel pipe body especially in the vicinity of the failure region as the pipe thickness reduces due to the corrosion/erosion effect. The study was performed by means of 3D and 2D structural simulation. The 3D failure study was conducted with an aim to identify and locating the maximum stress and maximum displacement at nominated punch area. The 2D structural simulation on the other hand will lead to a better understanding of the effect of pipe thickness reduction due to pipe erosion at failed area. It could also indicate the minimum wall thickness prior to structural rupture based on pipe wall strength analysis. Finally the pipe cross-section thickness mapping was studied to describe the thinning process that took place on the pipe outer surface. The thickness reduction occurs from the external corrosion/erosion effect could also be looked into.

6.2.1. Structural geometry

In order to provide better understanding of the real system modeling, the modeled geometry must actually resemble the real condition. Geometry for the pipe has been developed using 3D CAD (computer aided design) modeling, applying the following similarity factor:

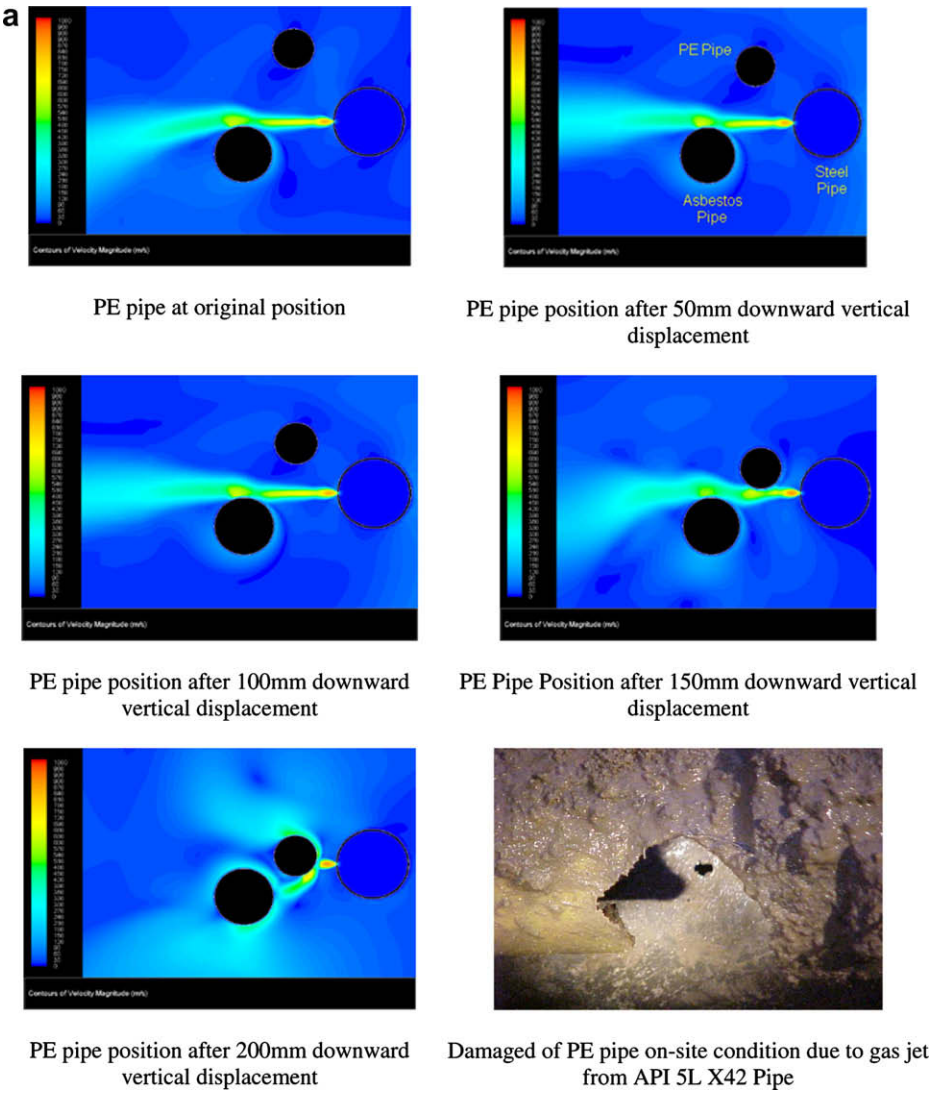

Fig. 19. Gas flow pressure and velocity contours for the API 5L pipe leak. (a) Gas pressure contours for the API 5L X42 pipe leak. (b) Gas flow velocity contours for the API 5L pipe leak.

b

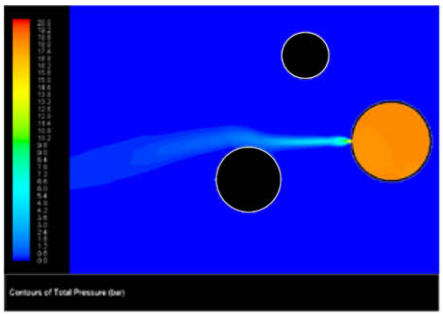

PE Pipe at original position

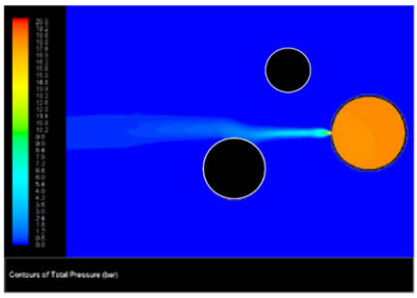

PE pipe position after 50mm downward vertical displacement

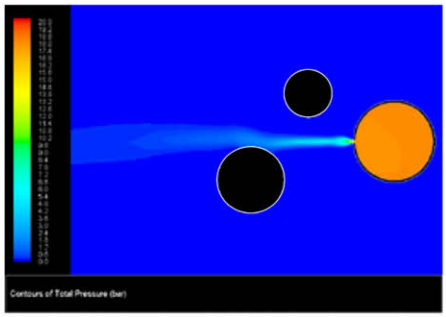

PE Pipe position after 100mm downward vertical displacement

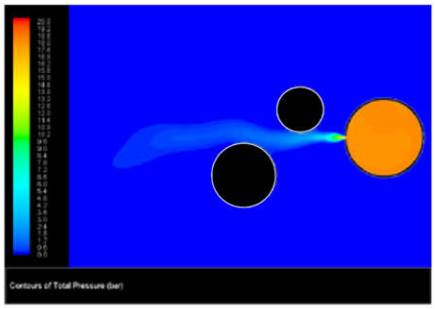

PE pipe position After 150mm downward vertical displacement

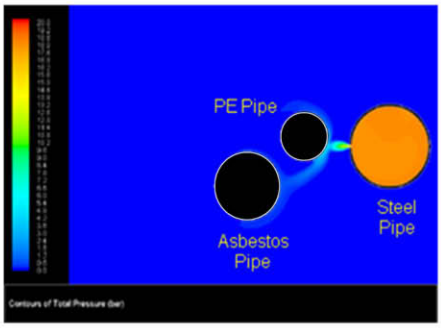

PE Pipe Position after 200mm downward vertical displacement

Damaged PE pipe on-site condition due to gas jet from API 5L X42 pipe

Fig. 19 (*continued*)

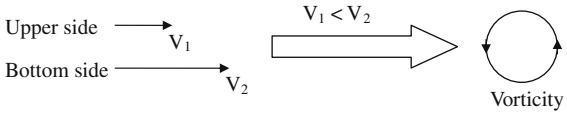

Fig. 20. Vorticity flow development.

i. Calculation conducted only to a portion of the NPS8 pipe domain of the modeled structure in order to reduce the meshing and analysis complexity. The pipe length used is 1000 mm (exceeding 20 pipe size diameter, >20D) where the effect or reaction at each end can be directly neglected.

ii. Carbon steel material was assumed homogeneous.
iii. The thickness of the pipe under consideration was assumed similar at any location (i.e. NPS8 = 5.6 mm).

6.2.2. FEA simulation results

Fig. 21 shows four samples of finite element simulation results obtained. Summary of results (Table 5) shows that as the punch depth gets deeper, the critical pressure due to the surface thickness reduction will subsequently increased. The critical element displacement also increased as the wall thickness is further reduced.

6.2.3. Results and discussion on wall thickness reduction

In the simulation process, 1800 kPa (18 bar) internal pressure was applied from inside the pipe structure. Using pipe thickness mapping, the pipe thickness is modeled and simulated for different cases. The pipe thickness dimension model has been based on its initial size of 5.8 mm. The simulations were subsequently executed for every 1 mm reduction of pipe thickness shown in Fig. 22.

Fig. 21 and Table 5 (3D analysis) represent pipe wall stress and displacement distribution, which indicate substantial increment as wall thickness reduces. The thickness reduction then lead to pipe failure is indicated by profile 7 (Fig. 22).

Results of 2D wall thickness reduction study are shown in Table 6, Figs. 23–25. It is clearly shown that the thickness reduction is directly due to the erosion effect. From the wall thickness profile, if the wall thickness is lower than 1.5 mm, the strength of the wall pipe is becoming weaker and the minimum thickness prior to failure is 1.25 mm limit.

Case 1: Stress Profile	Case 1: Displacement Profile
Punch Depth: 0 mm (Pipe in normal operating condition) Punch Radius: 0 mm Internal pressure: 1.8 MPa Max displacement: $46.6X10^6$ Pa	Punch Depth: 0 mm (Pipe in normal operating condition) Punch Radius: mm Internal pressure: 1.8 MPa Max displacement: 0.0202 mm
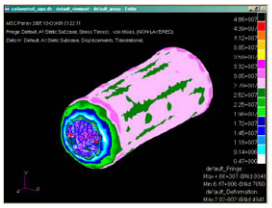	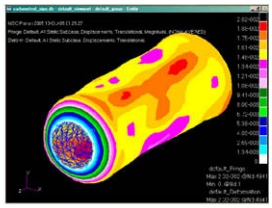
Case 2: Stress Profile	**Case 2: Displacement Profile**
Punch Depth: 2 mm Punch Radius: 1 mm Internal pressure: 1.8 MPa Max displacement: $47.4X10^6$ Pa	Punch Depth: 2 mm Punch Radius: 1 mm Internal pressure: 1.8 MPa Max displacement: 0.0206 mm
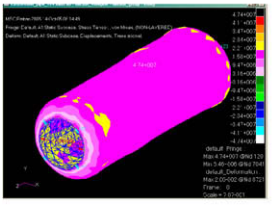	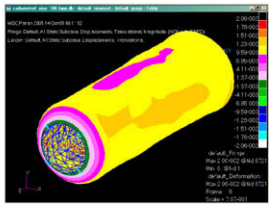

Fig. 21. Stress profile on API 5L X42 pipes.

Table 5
Summary of 3D simulation result.

Punch depth	Pipe thickness (mm)	Stress (MPa)	Displacement (10^{-2} mm)
Normal	5.6	46.6	2.02
2 mm	3.6	47.4	2.06
Hole	0	46.9	2.00

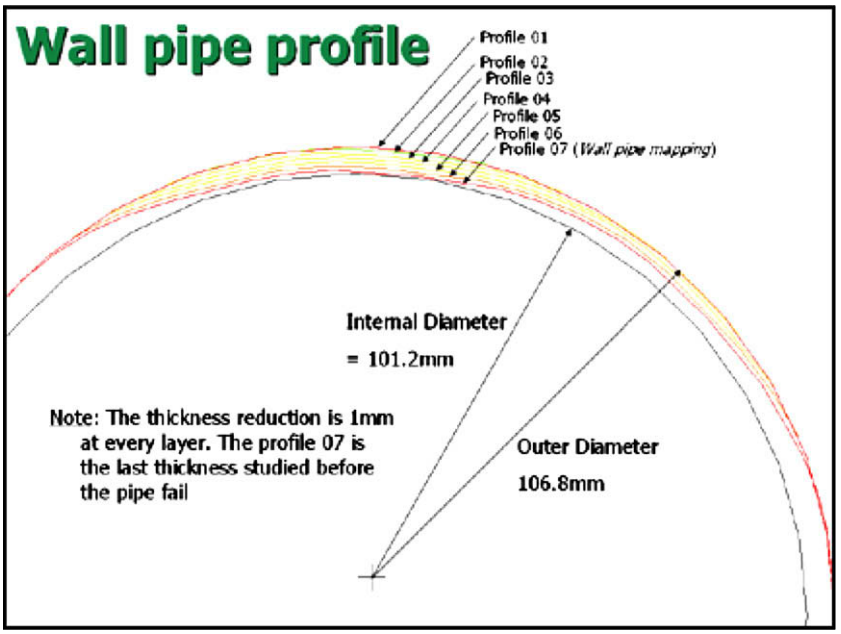

Fig. 22. Steel pipe wall profile.

6.2.4. Discussion on structural simulation results

Our study suggests that the asbestos water pipe with 10 mm wall thickness was the first to fail. It probably started with a small crack that could have produced the strong jetting effect that erodes rapidly the steel pipe. The flowing water pressure in the pipe was reported at around 1000 kPa (10 bar). The leak could have caused a high pressure water jet in which, with the presence of the surrounding soil and sand materials, could have produced highly abrasive slurry. This slurry could have impacted upon the NPS8, first causing the erosion of the coating materials and then the thinning of the steel pipe body. After sufficient pipe material was removed, the remaining pipe strength will no longer able to withstand the high internal pipe natural gas pressure. This eventually led to the steel pipe pinhole rupture and eventual enlargement, forcing more gas out of the pipe.

Ideas stating that the steel pipe has developed the first leak and caused the damage of the water pipe can easily be refuted. Photo evidence (Fig. 26) from the repositioning of the pipes showed that the steel pipe leak position is not directly facing the water pipe but rather towards the top. The opening of the water pipe is directly facing the eroded part of the steel pipe.

The high pressure jet of leaked water from the 6″ (152.4 mm) water pipe had earlier caused the displacement of the supporting soil materials underneath the MDPE causing it to move downwards. When the steel gas pipe leaked, more materials was displaced causing the MDPE pipe to drop even further until it was low enough to be '*in the line of fire*' from the high pressure gas jet. It was estimated that the MDPE pipe dropped some 200 mm from its original position.

7. Conclusions

In reference to the existing evidence deduced from the tests, simulation and substantial existing data the study revealed that the root cause of the pipe failures is attributed to the initial leak of the asbestos water pipe. The pattern of the water pipe

Table 6
Results on the pipe wall stress profile.

Profile	Stress (Pa)		
	Max. stress (von misses)	Permissible stress	Different
1	4.38E + 06	9.30E + 07	8.86E + 07
2	4.87E + 06	9.30E + 07	8.81E + 07
3	7.63E + 06	9.30E + 07	8.54E + 07
4	1.14E + 07	9.30E + 07	8.16E + 07
5	1.76E + 07	9.30E + 07	7.54E + 07
6	3.26E + 07	9.30E + 07	6.04E + 07
7	1.31E + 08	9.30E + 07	**3.80E + 07**

Note: bold number shows that the pipe has already failed when the maximum stress exceed the permissible stress.

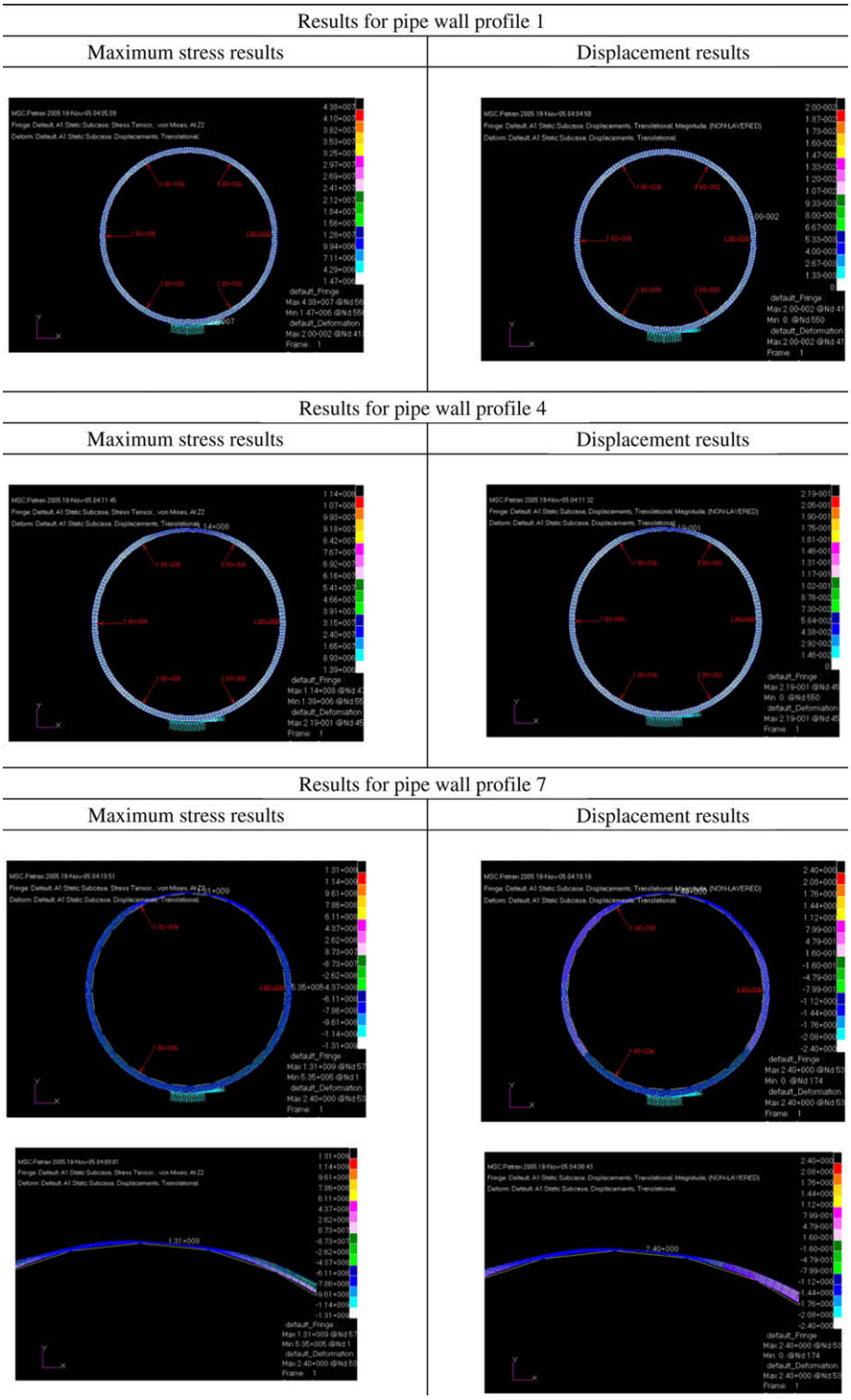

Fig. 23. Max stress and displacement results at pipe wall.

failure could not be determined due to the absence of damage specimen and the photo evidence at site only showed the state of the pipe after excavation. However, from the basic pipe material properties and behaviour, it is suspected that the failure was initiated by a crack, most probably longitudinal in nature. The crack or horizontal slit allowed high pressure water to jet

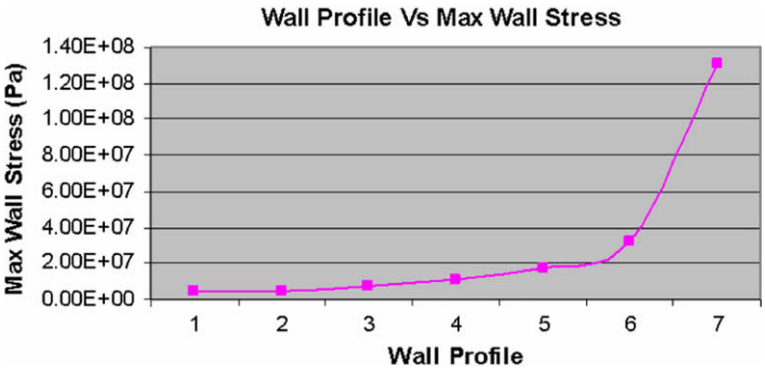

Fig. 24. Maximum stress.

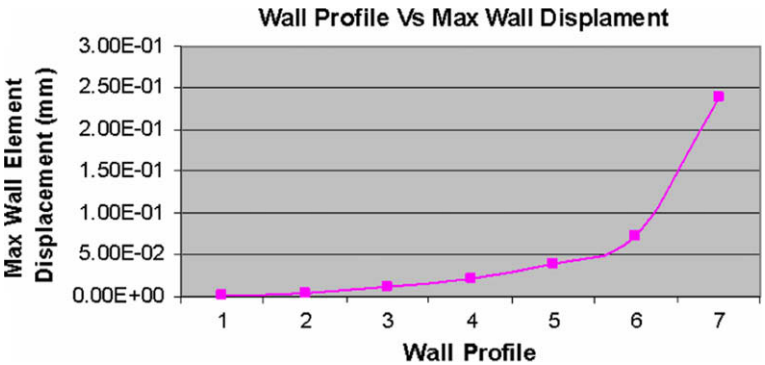

Fig. 25. Maximum displacement.

Fig. 26. Relative positions of the 8 in. water pipe to the NPS 8.

through, with the jet momentum getting stronger as the effective diameter of the slit increasing. Over time the crack enlarge and break off into large chunk or chunks, resulting in the gaping hole as evident in the photo record.

Initially, the water jet will mix with soil to form water slurry with high erosive properties. It impacted upon the pipe surface causing the loss of pipe coating materials. Corrosion quickly ensued and material loss was rapid because of the continuous erosion of oxidised material that occurred simultaneously. This phenomenon explains the rapid thinning of the steel pipe body which later led to its failure. The possibility of material defect on the NPS8 can be ruled out as clearly indicated by evidence from the metallurgical study especially on the photomicrograph. The morphology of the steel material was

consistent and did not show any evidence of micro fractures. Simulation results from both the CFD and structural study strongly support the stated hypotheses.

Acknowledgements

Authors are most grateful and wish to thank Dr. Ali Ourdjini, Mr. Mohd For Mohamad Amin and all members of Gas Technology Center (GASTEG) Pipeline Failure Team for their significant efforts and commitments in conducting experiments and simulation performing throughout research period. Gas Malaysia Sdn. Bhd (GMSB) and its staff are also highly acknowledged for providing pipe samples and continual financial support. Special thank is dedicated to Mr. Mohd Pozi Jusoh, the Operation and Maintenance Manager of GMSB for his continual support, ideas and commitment throughout the project period.

References

[1] Hassan F, Iqbal J, Ahmed F. Stress corrosion failure of high-pressure gas pipeline. Eng Fail Anal 2007;14:801–9.
[2] Hemandez-Rodridriguez MAL, Martinez-Delgado D, Gonzalez R, Perez Enzeta A, Mercado Solis RD, Rodriguez J. Corrosive wear failure analysis in a natural gas pipeline. Wear 2007;263:567–71.
[3] Shalaby HM, Riad WT, Alhazza AA, Behbehani MH. Failure analysis of fuel supply pipeline. Eng Fail Anal 2006;13:789–96.
[4] Azevedo CRF. Failure analysis of a crude oil pipeline. Eng Fail Anal 2006;13:789–96.
[5] Al-Bukhaiti MA, Ahmed SM, Bsdran FMF, Emara KM. Effect of impingement angle on slurry erosion behaviour and mechanism of 1017 steel and high-chromium white cast iron. Wear 2007;262:1187–98.
[6] Hamzah R, Stephenson DJ, Strutt JE. Erosion of materials used in petroleum production. Wear 2004;186:493–6.
[7] Aimin F, Jinming L, Ziyun T. Failure analysis of the impeller of slurry pump subjected to corrosive wear. Wear 1995;181–182:876–82.
[8] Haugen K, Kvernvold O, Ronold A, Sandberg R. Sand erosive of wear-resistance materials: erosion in choke. Wear 1995;186–187:179–88.
[9] National Transportation Safety Board. Pipeline incident report, natural gas pipeline rupture and fire, near carlsbad, New Mexico, August 19 2000. Virginia: National Technical Information Service; 2000.
[10] National Transportation Safety Board. Pipeline incident report, natural gas pipeline rupture and fire in south riding, Virginia, July 7 1998. Virginia: National Technical Information Service; 1998.
[11] Clark HMcI. Specimen diameter, impact velocity, erosion rate and particle density in a slurry pot erosion tester. Wear 1993;162–164:669–78.